Effect of severe plastic deformation by ECAP on corrosion behaviour of aluminium alloy AA 7075

M. Ilieva *, R. Radev

Department of Materials Science and Technology, Faculty of Mechanical and Manufacturing Engineering, University of Ruse, ul. Studentska 8, 7017 Ruse, Bulgaria

* Corresponding e-mail address: mdilieva@uni-ruse.bg

ABSTRACT

Purpose: The present study compares the corrosion behaviour of overaged AA 7075 before and after equal channel angular pressing ECAP in two media, containing chlorides, in order to answer the question how grain refinement of aluminium alloys influences their corrosion properties.

Design/methodology/approach: The effect of equal channel angular pressing ECAP on corrosion behaviour of aluminium alloy AA 7075 was studied in two water solutions, containing chloride ions: 1) 0.01 M Na_2SO_4 with addition of 0.01%Cl-, and 2) 3g/l H_2O_2 and 57g/l NaCl. The changes in electrochemical characteristics, provoked by grain size refinement after equal channel angular pressing ECAP, were found using potentiodynamic polarisation. Steady state potential, corrosion potential, corrosion current density; breakdown (pitting) potential of overaged and deformed by equal channel angular pressing ECAP aluminium alloy AA 7075 were measured.

Findings: In the environment with lower chloride concentration equal channel angular pressing ECAP process led to increase in pitting corrosion resistance and in the medium with higher chloride concentration - to decrease in pitting corrosion resistance. That way grain refinement does not demonstrate a uni-directional influence on corrosion resistance of AA 70775.

Research limitations/implications: The results suggest the possibility for development of materials having the same chemical composition but with different corrosion resistance to different environments.

Originality/value: The paper presents the corrosion behaviour of ultrafine-grained aluminium alloy AA 7075 and the influence of the chloride ions concentration in the corrosion medium on this behaviour.

Keywords: Metallic alloys; Aluminium alloys; Corrosion; Equal channel angular pressing

Reference to this paper should be given in the following way:

M. Ilieva, R. Radev, Effect of severe plastic deformation by ECAP on corrosion behaviour of aluminium alloy AA 7075, Archives of Materials Science and Engineering 81/2 (2016) 55-61.

MATERIALS

1. Introduction

Severe plastic deformation is known to lead to reduction in grain size of metallic materials to sub-micrometre levels, thus allows to obtain ultra-fine grained structure. The latter is characterised by increased strength, toughness and wear resistance. One of the widespread methods for severe plastic deformation of aluminium and its alloys is equal channel angular pressing (ECAP). The changes in microstructure and in mechanical properties after severe plastic deformation of Al and Al-alloys have drawn attention of a number of researchers [1-6]. Microstructural changes during severe plastic deformation will also alter corrosion behaviour, but there are sparing researches on that topic. Song et al. [7] investigated corrosion behaviour of ultra-fine grained pure Al in a chloride ion medium after ECAP and found improved resistance to pitting corrosion, attributed to more stable passive film due to the larger number of grain boundaries. Gopala et al. [8] also found improved corrosion resistance in chloride solutions of ultra-fine grained Al-4Zn-2Mg alloy, produced by cryorolling. Birbilis et al. [9] and Gollapudi [10] summarised research results for corrosion rates as a function of grain size and Gollapudi [10] as a function of grain size distribution. They suggested that the change in grain size does not have a uni-directional influence on corrosion resistance, but the capabilities of medium to passivate govern the presence of a surface passive layer and its response to medium. Materials with the same chemical composition could show an improvement in corrosion behaviour with grain refinement when they are in contact with a passivating medium, or a decrease in corrosion resistance when the environment is active. In the case of a medium that has simultaneously an active action and a passivating action, grain refinement leads to increase in resistance to localised corrosion degradation, but is favourable for uniform corrosion.

The present study compares the corrosion behaviour of overaged AA 7075 before and after ECAP in two media, containing chlorides, using potendidynamic polarisation.

2. Materials and methods

2.1. Materials

The studied specimens were prepared from AA 7075 aluminium alloy by equal angular channel pressing (ECAP). The deformation process for studied samples from

AA 7075 was carried out together with deformation of three other aluminium alloys: AA 1050, AA 5005 and AA 6082 [11].

Electron Probe MicroAnalysis on JEOL JXA-733 Superprobe indicated the composition of AA 7075 samples, shown in Table 1.

Table 1
Chemical composition of AA 7075

Chemical composition wt. %						
Si	Fe	Mg	Cu	Zn	Mn	Al
0.24	0.35	2.87	1.83	5.59	0.03	remainder

In order to prevent the influence of the previous thermal or mechanical processes, all samples were overaged before the ECAP process. The temperature for heat treating of AA 7075 was 343°C, followed by controlled cooling down to 230°C, holding for 4 hours at this temperature and cooling in air.

After the heat treatment, the ECAP process was applied. Schematic illustration of the ECAP procedure and 3D drawing of ECAP tool are shown in Figure 1. The tool for AA 7075 deformation was with $\varphi = 60°$ and six passes were made. The temperature during ECAP was $T = 20°C$. More detailed description of the deformation process can be found in [11]. Metallographic examination of studied AA 7075 samples was not carried out, but for AA 1050 specimens, and showed sub-micrometre grain size, characteristic for ultra-fine grained (UFG) materials [11]. As AA 1050 also was deformed in six passes, it can be considered that after deformation of AA 7075 its structure is ultra-fine grained.
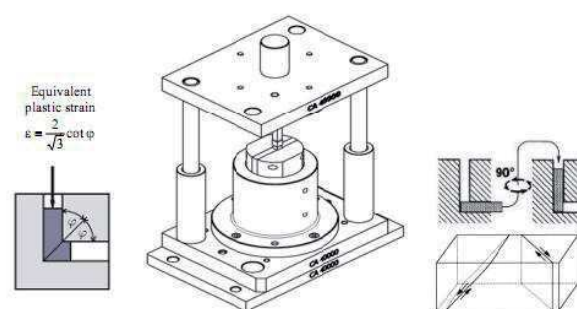

Fig. 1. Schematic c of the ECAP process, 3D drawing of ECAP tool set, deformation sequence and shear planes at each deformation pass [11]

2.2. Corrosion tests

The specimens, which were cut from the deformed billets of AA 7075, in the present text, are denoted as deformed. Their behaviour was compared with that of overaged specimens, which were cut from the heat-treated billets of AA 7075. They are denoted as heat treated or overaged.

Potentiodynamic polarisation tests [12-17] were carried out at room temperature in two open to air solutions: 1) a sodium sulphate solution: 0.01 M Na_2SO_4 with addition of 0.01%Cl^- (0.17 g/l NaCl or 0.03 M NaCl) [7] and 2) a hydrogen peroxide solution: 3 g/l H_2O_2 and 57 g/l NaCl [18]. These media have an active component - chloride ions, that attack the naturally formed passive oxide layer on top of Al and Al-alloys. Passivating component for H_2O_2 solution is the dissolved in the solution oxygen, as the aluminium alloys, containing copper, catalyse the decomposition of hydrogen peroxide [18]. For Na_2SO_4 solution SO_4^{2-} ions imitate a passivating environment as they absorb on top of the Al_2O_3 layer and impede the chloride ions penetration, and thus – the pits initiation, but when pits are present, sulphate ions facilitate the corrosion process [19].

Before electrochemical corrosion tests, all samples were polished, washed and degreased. The analysed surface area was 0.4 cm^2. A saturated calomel electrode (SCE) was used as a reference electrode. All values of potentials were calculated versus standard hydrogen electrode (SHE), accounting experiment temperature, at which SCE has a potential of +245 mV. Potentiodynamic polarisation was performed using standard three electrode cell with a Pt-electrode as a counter electrode, SCE as a reference electrode and the studied sample as a working electrode. The external polarisation potentials were applied with a potentiostat RADELKIS OH-405. The data from tests were collected with a USB digital acquisition controller NI USB-6008 and then were plotted as graphs.

Before the polarisation, all specimens were allowed to stabilise for a period of 60 minutes. Meantime variations in open circuit potentials (OCP) were recorded as a function of time. At the end of that period all samples reached steady state potentials E_{ss}. Immediately after that potentiodynamic polarisation was performed. The scan rate was 1 mV/s. The polarisation potentials were changing from -750 mV/SHE to +900 mV/SHE for sodium sulphate solution, and from -750 mV/SHE to -300 mV/SHE for hydrogen peroxide solution. Using Tafel extrapolation, corrosion current densities i_{corr} and corrosion potentials E_{corr} were determined from potentiodynamic polarisation curves. Corrosion potential was determined as the potential, at

which the current density changes from cathodic to anodic [8]. For samples, tested in sodium sulphate solution, breakdown (pitting) potentials E_{pit} were determined from polarisation curves as the points in the anodic branches of curves, at which a sharp increase in current density is observed.

3. Results and discussion

In sodium sulphate solution, the open circuit potential of heat treated sample did not vary with more than 10 mV over time (Figure 2). This indicates that a variation in oxide layer did not occur. The deformed specimen showed initial increase in OCP and then OCP dropped to almost constant value. That is an indication for an initial modification in the protective oxide layer on top of the deformed metal [18] in Na_2SO_4 solution. Steady state potentials E_{ss} of both specimens were close in value. The difference in E_{ss} is 24 mV and more positive value was measured for deformed specimen (Table 2). Hydrogen peroxide solution shifted OCP and E_{ss} values to more negative than measured in sodium sulphate solution (Figure 3 and Table 3).
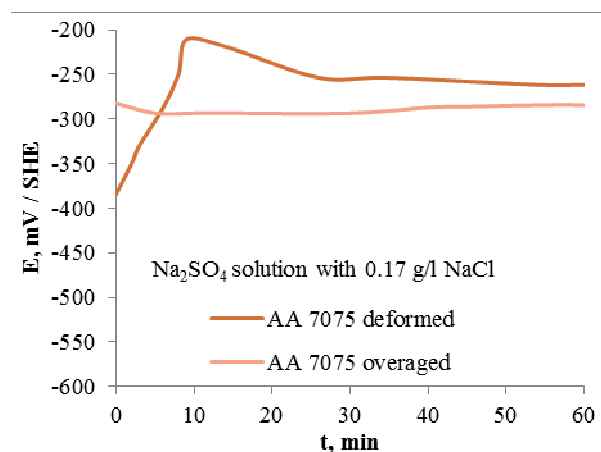

Fig. 2. Open circuit potentials as a function of time in Na_2SO_4 solution

The values of OCP in Na_2SO_4 solution did not alter with more than 8 mV over time – the oxide layers on both specimens remained unchanged. Whereas in Na_2SO_4 solution the deformed specimen showed greater E_{ss} than heat treated one, in H_2O_2 solution its steady state potential was more negative than measured for heat treated sample. The difference in E_{ss} in H_2O_2 solution is bigger: 72 mV.

Table 2.

Electrochemical properties of studied samples: in sodium sulphate solution: E_{ss} – steady state potential; E_{corr} – corrosion potential; i_{corr} – corrosion current density; E_{pit} – breakdown (pitting) potential

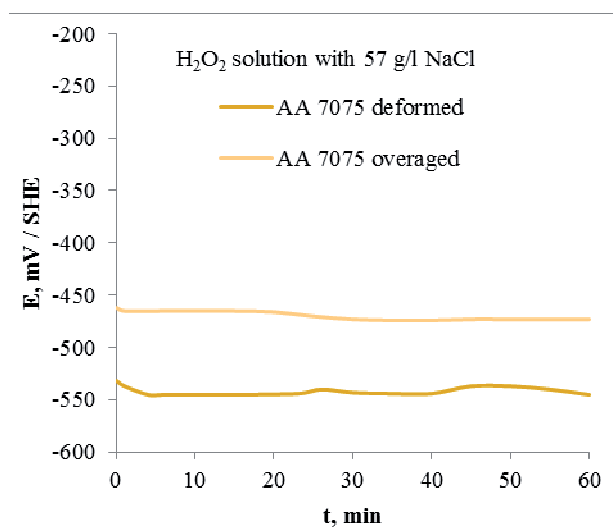| AA 7075	Na_2SO_4 solution with 0.17 g/l NaCl			
	E_{ss}, mV	E_{corr}, mV	E_{pit}, mV	i_{corr}, mAcm^{-2}
Overaged	-286	≈-300	-180	0.0017
Deformed	-262	≈-300	-123	0.0015

Fig. 3. Open circuit potentials as a function of time in H_2O_2 solution

Table 3.

Electrochemical properties of studied samples: in hydrogen peroxide solution: E_{ss} – steady state potential; E_{corr} – corrosion potential; i_{corr} – corrosion current density

AA 7075	H_2O_2 solution with 57 g/l NaCl		
	E_{ss}, mV	*E_{corr}, mV	i_{corr}, mAcm^{-2}
Overaged	-473	-453	0,04
Deformed	-545	-506	0,12

*E_{corr} and E_{pit} coincide

Potentiodynamic polarisation curves (PDCs) of the studied specimens in both solutions (Figure 6 and Figure 7) are typical for aluminium and its alloys – PDCs do not demonstrate domain of passivity as aluminium and its alloys are naturally passive [18]. Potentiodynamic curves indicate better behaviour of studied samples when they were immersed and polarised in the solution with the lower chloride concentration (Na_2SO_4 solution). Corrosion potentials (E_{corr}) and corrosion current densities (i_{corr}) were determined from PDCs (Table 2 and Table 3). Their values also confirm the superior behaviour of both samples in Na_2SO_4 solution. In sodium sulphate solution, all PDCs are shifted towards current densities, lesser than 10 mA/cm^2 over all applied range of polarisation, and towards less negative corrosion potentials. That position of PDCs is due to the lower chloride concentration in sodium sulphate solution.

Corrosion potentials and corrosion current densities in Na_2SO_4 solution suggest a better behaviour for deformed specimen. However, the values of E_{corr} and i_{corr} are close. These facts indicate that, near the corrosion potentials, used deformation did not influence the response of protective oxide layer on AA 7075 to sodium sulphate solution, and therefore, the behaviour of AA 7075 at polarisation near corrosion potentials. However, anodic polarisation in Na_2SO_4 solution, following corrosion potentials, led to breakdowns in the passive films on both specimens and to higher anodic current densities for heat treated sample. Those breakdowns are characterised by pitting potentials E_{pit}, given in Table 2. After external polarisation, few shallow pits were observed on heat treated surface, whereas deformed specimen did not show any visible (macroscopic) pits but only blackening (Figure 4 and Figure 5). The observed pits and the breakdowns on PDCs in the Na_2SO_4 solution show that the sulphate ions concentration was insufficient to demonstrate its inhibitive effect on AA 7075 corrosion (Fig. 6), which was reported by [20].

Fig. 4. Appearance of the tested in Na_2SO_4 solution overaged sample-few pits can be seen

The more negative value of E_{pit} and the higher anodic current densities of heat treated specimen reveal the influence of grain refinement on corrosion behaviour. Severe plastic deformation caused grain refinement thus increased grain boundaries and dislocations density. It is known that high density of grain boundaries and of

dislocations provides sites, susceptible for passive layer formation [7,10,21]. Therefore, more stable and uniform passive film formed on top of deformed specimen and that film defined its more positive breakdown potential and smaller anodic current densities at more positive polarisation potentials. As OCP change shows, in the first ten minutes of the test the oxide layer on top of the deformed specimen reacted with the solution to become even more stable (Figure 2). When the oxide film formed on heat treated surface with coarser grains, it was less uniform [7,10] and in the contact with the solution it did not undergo a variation in OCP. The underneath metal of heat treated specimen was barer to local anodic dissolution when greater potentials were applied.

Fig. 5. Appearance of the tested in Na_2SO_4 solution deformed sample-only blackening is observed
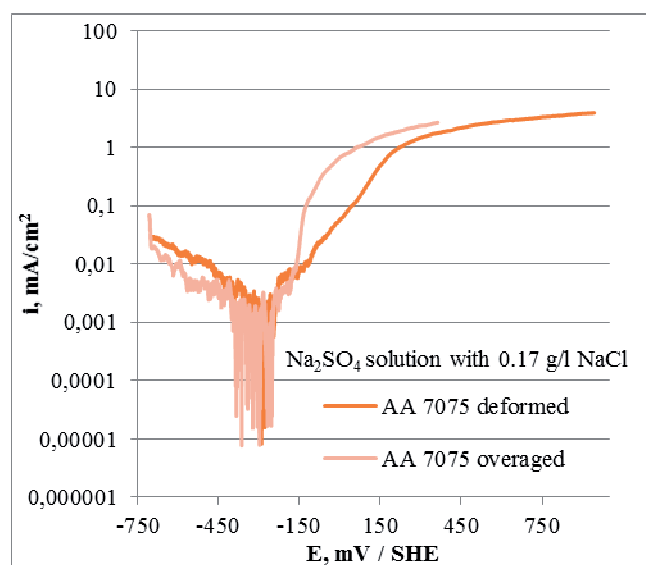

Fig. 6. Potentiodynamic polarisation curves in Na_2SO_4 solution

On potentiodynamic curves (Figure 7) in H_2O_2 solution breakdowns are missing. According to [18], the absence of breakdown on potentydinamic curves indicates that the corrosion and pitting potentials have close values, i.e. the breakdown coincides with the pitting potential. As the chloride ions concentration in peroxide solution is higher than that in sulphate solution, the higher cathodic and anodic current densities are result from localised corrosion processes, leading to pits formation [22].
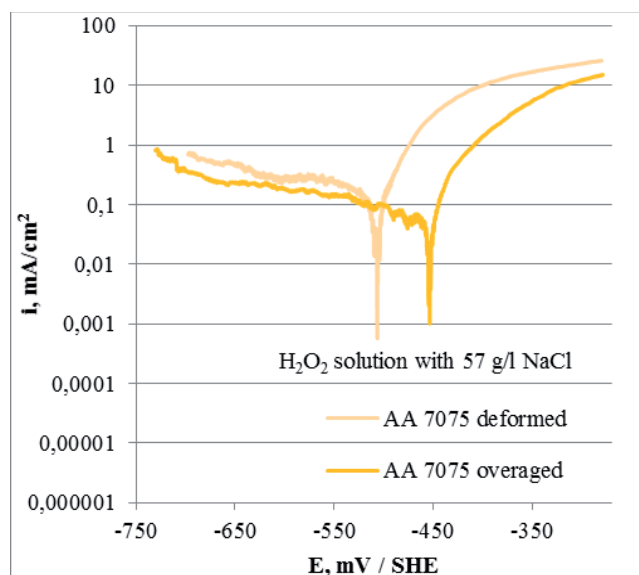

Fig. 7. Potentiodynamic polarisation curves in H_2O_2 solution

Alloy AA 7075, as all 7xxx series aluminium alloys, catalyses the decomposition of H_2O_2 [18] and that way increases the dissolved oxygen concentration. Oxygen, dissolved in the solution, has a bi-directional influence on aluminium alloys corrosion: 1) it takes part in the depolarisation reaction, promoting the corrosion process, and 2) it contributes to oxide layer formation and growth, thus slows down metal dissolution. The high current densities, measured from PDCs (Figure 7), indicate that the repassivation, due to dissolved oxygen, was not sufficient to fully compensate depassivation, caused by chloride ions.

In H_2O_2 solution the deformed specimen, compared with the heat treated one, demonstrated one order higher corrosion current density at 53 mV more negative corrosion/pitting potential (Table 3). Anodic and cathodic current densities of the deformed sample were also greater than these of the heat treated. As the density of grain boundaries increased after severe plastic deformation, overall surface chemical activity also increased [8,9], i.e.

more elementary acts of oxide film depassivation by chloride ions occurred on deformed surface than on top of heat treated specimen. That way the deformed (fine grained) structure demonstrated lower corrosion resistance to pitting corrosion in hydrogen peroxide solution than the coarse-grained structure.

In [9] is proposed dependence similar to that of the Hall-Petch that describes influence of the grain size d on the current density of corrosion i_{corr} (proportional to the rate of corrosion) – Figure 8 and Figure 9:

$$i_{corr} = a + bd^{-0.5} \qquad (1)$$

In this relationship a and b are constants that take into account:
1) type of environment;
2) type of metal;
3) chemical composition of corroded metal/alloy.

Slope b is positive in non-passivating (active) environments and negative - in passivating. Thus, dependence (1) shows that in the presence of a passive oxide layer, the reduction of the grain size would lead to a reduction of the corrosion rate. In the absence of a passive layer the fine-grained structures will undergo corrosion with a higher speed than the coarse-grained.
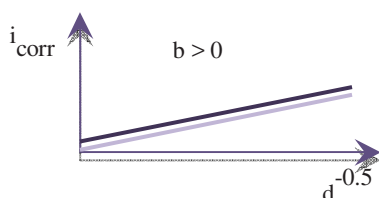

Fig. 8. Effect of environment and grain size on the rate of corrosion of metals and metal alloys in an active medium
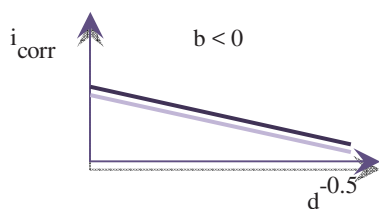

Fig. 9. Effect of environment and grain size on the rate of corrosion of metals and metal alloys in an passivating medium

According to [10], in an environment with both activating and passivating action, reducing the size of the grains will cause higher rates of general corrosion and lower – of the local types of corrosion. The described by the relationship (1) influence of the type of environment on the rate of corrosion may be explained by the impact of the environment on the passivating behaviour of the specific metal. Obviously, the increased boundaries and dislocations densities in the passivating environment advantage the transition into a passive state and the maintenance of this state (due to easy generation of a passive layer on the grain boundaries and dislocations outputs of the surface). The increased surface energy, that is a result from increased boundaries and dislocations densities, leads to increased surface activity and – to dissolution with greater rate in environments that degrade the passive layer or prevent its formation. Bidirectional influence of intensive plastic deformation on the corrosion resistance of metallic materials necessitates extensive corrosion studies to determine the corosion behaviour of ultra-fine grained metals in different environments.

The corrosion behaviour of the studied here aluminium alloy AA 7075 is dependent on the environment and on the grain size. As after ECAP the grain size is reduced to sub-micrometre grain scale, the tendency to localised corrosion in the medium, deficient in depassivating chloride ions, decreases. The medium, abundant in chloride ions, accelerates the rate of localised corrosion. These findings are in accordance with the described in the literature effects of environment and grain size on the rate of corrosion of metals and metal alloys.

4. Conclusions

When the specimens were immersed in Na_2SO_4 solution with lower chloride concentration, steady state potentials, corrosion potentials and corrosion current densities, and hence, corrosion rates, were unaffected by the deformation process. The deformed specimen was less susceptible to pitting corrosion and showed smaller rates of localised (pitting) corrosion than the heat treated one.

In H_2O_2 solution with higher chloride concentration the deformation process of AA 7075 led to more negative steady state potentials, more negative corrosion potentials and increased with one order corrosion current density, meaning increased corrosion rate. These facts confirm that grain refinement does not have uni-directional influence on the corrosion rate of AA 7075.

The results suggest the possibility for development of materials having the same chemical composition but with different corrosion resistance in different environments.

References

[1] G.Z. Quan, Y.P. Mao, G.S. Li, W.Q. Lv, Y. Wang, J. Zhou, A characterization for the dynamic recrystallization kinetics of as-extruded 7075 aluminum alloy based on true stress-strain curves, Computer Materials Science 55 (2012) 65-72.

[2] O. Senkov, F. Froes, V. Stolyarov, R. Valiev, J. Liu, Microstructure of Aluminum-Iron Alloys Subjected to Severe Plastic Deformation, Scripta Materialia 38 (1998) 1511-1516.

[3] F.X. Zhao, X.C. Xu, H.Q. Liu, Y.L. Wang, Effect of annealing treatment on the microstructure and mechanical properties of ultrafine-grained aluminum, Materials Design 53 (2014) 262-268.

[4] P.N. Rao, D. Singh, R. Jayaganthan, Mechanical properties and microstructural evolution of Al 6061 alloy processed by multidirectional forging at liquid nitrogen temperature, Materials Design 56 (2014) 97-104.

[5] K. Ma, H. Wen, T. Hu, T.D. Topping, D. Isheim, D.N. Seidman, et al., Mechanical behaviour and strengthening mechanisms in ultrafine grain precipitation-strengthened aluminum alloy, Acta Materialia 62 (2014) 141-155.

[6] R. Procházka, J. Džugan, M. Kövér, Miniature specimen tensile testing of AZ31 alloy processed by ECAP, Archives of Materials Science and Engineering 76/2 (2015) 134-139.

[7] D. Song, A. MA, J. Jiang, P. Lin, D. Yang, Corrosion behaviour of ultra-fine grained industrial pure Al fabricated by ECAP, Transactions of Nonferrous Metals Society of China 19 (2009) 1065-1070.

[8] K. Gopala Krishna, K. Sivaprasad, T.S.N. Sankara Narayanan, K.C. Hari Kumar, Localized corrosion of an ultrafine grained Al-4Zn-2Mg alloy produced by cryorolling, Corrosions Science 60 (2012) 82-89.

[9] K.D. Ralston, N. Birbilis, C.H.J. Davies, Revealing the relationship between grain size and corrosion rate of metals, Scripta Materialia 63 (2010) 1201-1204.

[10] S. Gollapudi, Grain size distribution effects on the corrosion behaviour of materials, Corrosions Science 62 (2012) 90-94.

[11] R. Radev, V. Gagov, D. Gospodinov, E. Yankov, Metal forming simulation of ultrafine-grained commercial pure aluminum, Euromat 39 (2011) 1.

[12] T. Liptáková, M. Lovíšek, B. Hadzima, S. Dundeková, Material parameters affecting degradation processes of Al-brasses in pipe systems, Archives of Materials Science and Engineering 76/1 (2015) 27-34.

[13] M. Dziekońska, A. Ziębowicz, B. Ziębowicz, L.A. Dobrzański, Corrosion resistance of neodymium composite materials reinforced with metal powders, Archives of Materials Science and Engineering 58/2 (2012) 137-145.

[14] L.A. Dobrzański, Ł. Reimann, C. Krawczyk, Effect of age hardening on corrosion resistance and hardness of CoCrMo alloys used in dental engineering, Archives of Materials Science and Engineering 57/1 (2012) 5-12.

[15] M. Kciuk, A. Kurc-Lisiecka, The influence of heat treatment on structure, mechanical properties and corrosion resistance of steel X10CrNi18-8, Archives of Materials Science and Engineering 55/2 (2012) 62-69.

[16] W. Walke, E. Hadasik, J. Przondziono, D. Kuc, I. Bednarczyk, G. Niewielski, Plasticity and corrosion resistance of magnesium alloy WE43, Archives of Materials Science and Engineering 51/1 (2011) 16-24.

[17] W. Kajzer, M. Kaczmarek, A. Krauze, J. Marciniak, Surface modification and corrosion behaviour of Ni-Ti alloy used for urological implants, Archives of Materials Science and Engineering 28/9 (2007) 525-532.

[18] C. Vargel, M. Jacques, M.P. Schmidt, Corrosion of Aluminium, Corrosions Aluminium 6 (2004) 81-109.

[19] W. Lee, S. Pyun, Effects of sulphate ion addition on the pitting corrosion of pure aluminium in 0.01 M NaCl solution, Electrochemia Acta 45 (2000) 1901-1910.

[20] T.I. Wu, J.K. Wu, Effect of Sulfate Ions on Corrosion Inhibition of AA 7075 Aluminum Alloy in Sodium Chloride Solutions, Corrosion 51/3 (1995) 185-190.

[21] M. Abdulstaar, M. Mhaede, L. Wagner, M. Wollmann, Corrosion behaviour of Al 1050 severely deformed by rotary swaging, Materials Design 57 (2014) 325-329.

[22] E. Ghali, Corrosion resistance of aluminum and magnesium alloys: understanding, performance, and testing, Wiley, 2010.